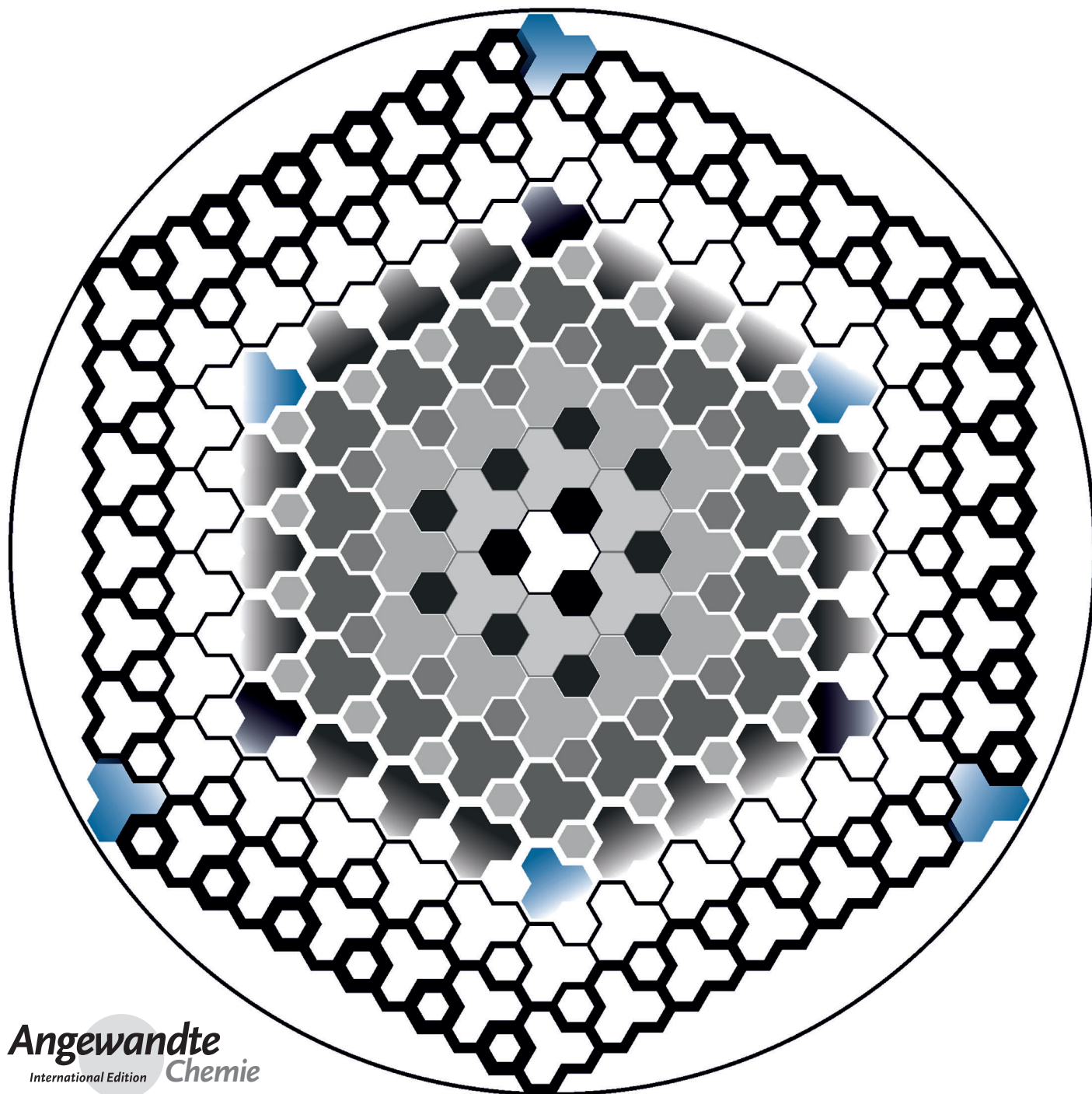




Triazine-Based Graphitic Carbon Nitride: a Two-Dimensional Semiconductor**

Gerardo Algara-Siller, Nikolai Severin, Samantha Y. Chong, Torbjörn Björkman, Robert G. Palgrave, Andrea Laybourn, Markus Antonietti, Yaroslav Z. Khimyak, Arkady V. Krasheninnikov, Jürgen P. Rabe, Ute Kaiser, Andrew I. Cooper,* Arne Thomas, and Michael J. Bojdys*



Abstract: Graphitic carbon nitride has been predicted to be structurally analogous to carbon-only graphite, yet with an inherent bandgap. We have grown, for the first time, macroscopically large crystalline thin films of triazine-based, graphitic carbon nitride (TGCN) using an ionothermal, interfacial reaction starting with the abundant monomer dicyandiamide. The films consist of stacked, two-dimensional (2D) crystals between a few and several hundreds of atomic layers in thickness. Scanning force and transmission electron microscopy show long-range, in-plane order, while optical spectroscopy, X-ray photoelectron spectroscopy, and density functional theory calculations corroborate a direct bandgap between 1.6 and 2.0 eV. Thus TGCN is of interest for electronic devices, such as field-effect transistors and light-emitting diodes.

Since the advent of single, free-standing 2D sheets of graphite,^[1] graphene has been suggested as the most promising candidate material for post-silicon electronics.^[2] Most notably, graphene has the desirable combination of high charge-carrier mobility coupled with high current stability, temperature stability, and thermal conductivity.^[3] However, the (semi-)metallic character of graphene and the absence of an electronic bandgap have so far impeded the development of a graphene-based switch.^[4] Strategies to open up a graphene bandgap involve single- or multi-step modifications by physical and chemical means.^[5] Alternative, simpler routes to silicon-free electronic switches are based on known inherent semiconductors. For example, a field-effect transistor was constructed using single-layer MoS₂ (1.8 eV bandgap) obtained by Scotch tape exfoliation, but this strategy retains the known chemical limitations of MoS₂.^[6] It is therefore desirable to complement the electronic properties of the carbon-only graphite/graphene system with a similar material that combines 2D atomic crystallinity and inherent semiconductivity.

The new material discussed here consists exclusively of covalently-linked, sp²-hybridized carbon and nitrogen atoms.

It was first postulated by others as “graphitic carbon nitride” (“g-C₃N₄”), by analogy with the structurally related graphite.^[7] Over the years, two structural models emerged to account for the geometry and stoichiometry of this as yet hypothetical graphitic carbon nitride. These two models are distinguished by the size of the nitrogen-linked aromatic moieties that make up the individual sheets in the material: one model is based on triazine units (C₃N₃) (Figure 1F and Figure S1 in the Supporting Information), and the other is based on heptazine units (C₆N₇) (Figure S1).^[8] Since the 1990s, many attempts at the synthesis of carbon nitride materials have been reported,^[8] encompassing chemical vapor deposition (CVD),^[9] pyrolysis of nitrogen-rich precursor molecules,^[10] shock wave synthesis,^[11] and ionothermal condensation.^[12] Historically, the existence of a hypothetical, heptazine-based “graphitic carbon nitride (g-C₃N₄)” has been claimed numerous times.^[10a,12–13] Later work revealed these materials to be either polymeric (CN_xH_y),^[14] or of a poly-(triazine imide)-type,^[15] and none of these approaches has yielded, up to now, a well-defined material of the postulated “g-C₃N₄” triazine structure. The electronic and chemical properties of these materials remain of strong interest: for example, recently a heptazine-based, disordered, more polymeric carbon nitride was shown to facilitate hydrogen evolution from water under visible-light irradiation.^[16] The present contribution now reports the successful surface-mediated synthesis of 2D crystalline, macroscopic films of triazine-based, graphitic carbon nitride (TGCN). The material forms interfacially, both at the inherent gas–liquid interface in the reaction and on a quartz glass support.

The principal synthetic procedure is analogous to the previously reported synthesis of poly(triazine imide) with intercalated bromide ions (PTI/Br).^[15a] In a typical experiment, the monomer dicyandiamide (DCDA) (1 g, 11.90 mmol) is ground with a vacuum-dried, eutectic mixture of LiBr and KBr (15 g; 52:48 wt %, m.p. 348 °C) in a dry environment to prevent adsorption of moisture. The mixture

[*] G. Algara-Siller, Prof. Dr. U. Kaiser
Universität Ulm, Materialwissenschaftliche Elektronenmikroskopie
Albert-Einstein-Allee 11, 89081 Ulm (Germany)

Dr. N. Severin, Prof. Dr. J. P. Rabe
Humboldt-Universität zu Berlin, Department of Physics & IRIS
Adlershof, Newtonstr. 15, 12489 Berlin (Germany)

S. Y. Chong, A. Laybourn, Prof. A. I. Cooper, Dr. M. J. Bojdys
University of Liverpool, Department of Chemistry and Centre for
Materials Discovery, Crown Street, Liverpool, L69 7ZD (UK)
E-mail: aicooper@liverpool.ac.uk
m.j.bojdys.02@cantab.net

Dr. T. Björkman
COMP/Department of Applied Physics, Aalto University
P.O. Box 11100, 00076 Aalto (Finland)

Dr. R. G. Palgrave
University College London, Department of Chemistry
20 Gordon Street, London, WC1H 0AJ (UK)


Prof. Dr. M. Antonietti
Max Planck Institute of Colloids and Interfaces
Department of Colloids
Am Mühlenberg 1, OT Golm, 14476 Potsdam (Germany)

Prof. Y. Z. Khimyak
School of Pharmacy, University of East Anglia
Norwich Research Park, Norwich, NR4 7TJ (UK)

Dr. A. V. Krashennnikov
Department of Applied Physics, Aalto University
P.O. Box 1100, 00076 Aalto (Finland)

Prof. Dr. A. Thomas
Technische Universität Berlin, Institute of Chemistry
Hardenbergstr. 40, 10623 Berlin (Germany)

[**] The authors thank EPSRC for funding (EP/H000925). M.J.B. is holder of a DAAD research fellowship. T.B. and A.V.K. acknowledge financial support by the Academy of Finland through Projects No. 218545 and No. 263416 and also thank CSC Finland for generous grants of computer time. A.T. acknowledges the European Research Council for financial support within the project 278593_ORGZEO. M.A. acknowledges the Project “Light2Hydrogen” of the BMBF (03IS2071D). N.S. and J.P.R. acknowledge support by the Helmholtz-Energie-Allianz. We thank Diamond Light Source for access to beamline I11 (EE7040) that contributed to the results presented in the Supporting Information.

 Supporting information for this article (including crystallographic information (CIF)) is available on the WWW under <http://dx.doi.org/10.1002/anie.201402191>.

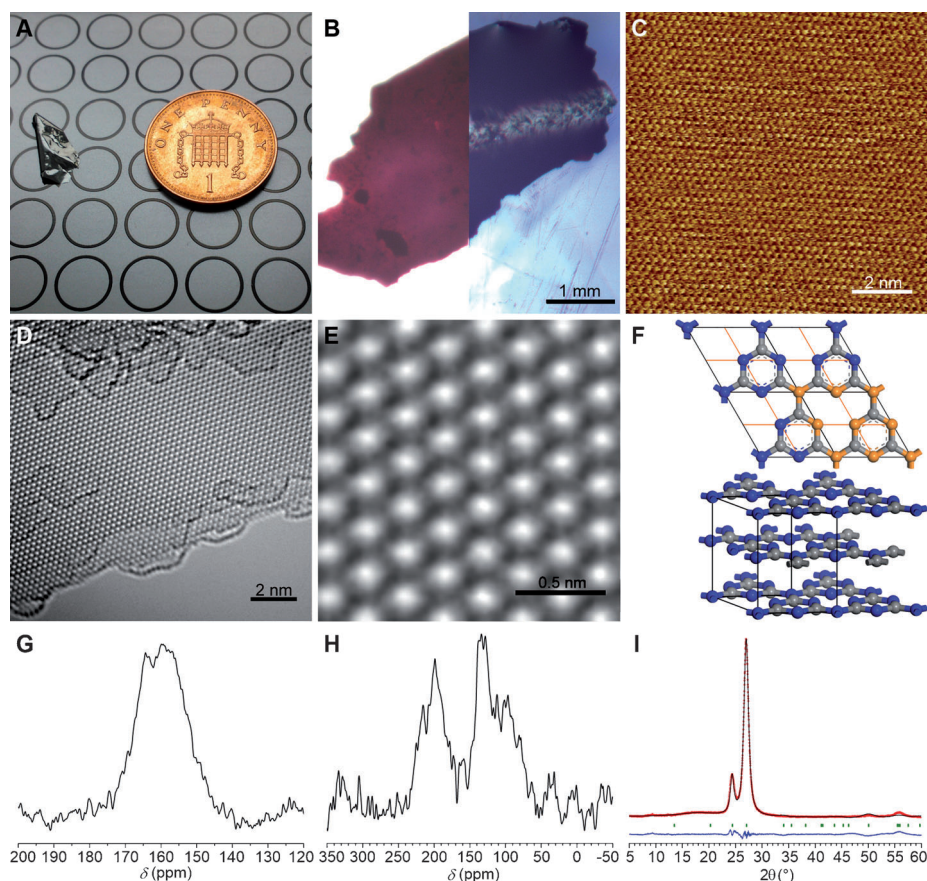


Figure 1. Physical characterization of TGCN. A) A single macroscopic flake of TGCN. B) Optical microscopy images of TGCN in transmission (left half) and reflection (right half). C–E) Mechanically cleaved layers of TGCN as imaged by SFM (C) and by high-resolution TEM (D and E). F) Crystallographic unit cell ($a = 5.0415(10)$ Å, $c = 6.57643(31)$ Å, space group 187) and AB stacking arrangement of TGCN layers derived from structural refinement. Carbon and nitrogen atoms are represented as gray and blue spheres, respectively. A hexagonal grid of half-cell size with nitrogen atoms at its nodes has been overlaid as guide for the eye in orange. G,H) ^{13}C $\{^1\text{H}\}$ magic-angle spinning (MAS) NMR (MAS rate of 10 kHz) (G) and ^1H - ^{15}N CP/MAS NMR spectra (MAS rate of 5 kHz, reference glycine) (H) of TGCN. I) X-ray analysis of TGCN with the observed pattern in red, the refined profile in black, the difference plot in blue, and Bragg peak positions in green.

is sealed under vacuum in a quartz glass tube ($l = 120$ mm, outer diameter = 30 mm, inner diameter = 27 mm) and subjected to the following heating procedure: 1) heating at 40 K min^{-1} to 400°C (4 h), 2) heating at 40 K min^{-1} to 600°C (60 h). **Safety note:** Since ammonia is a by-product of this polycondensation reaction, pressures in the quartz ampoule can reach up to 12 bar, so special care should be taken in handling and opening of the quartz ampoules. The reaction yields two products: PTI/Br, which is suspended in the liquid eutectic,^[15a] and a continuous film of TGCN at the gas–liquid and solid–liquid interface in the reactor. The size of the deposited TGCN flakes scales with the initial concentration of DCDA in the reaction medium, and with the reaction time. Hence, a low initial concentration of the monomeric building blocks (0.5 g DCDA in 15 g LiBr/KBr) yields isolated, transparent flakes of orange-red color (< 2 mm), as do shorter reaction times (< 24 h). By contrast, a combination of longer reaction times (> 48 h) and higher concentrations (1 g DCDA in 15 g LiBr/KBr) of monomer gives macroscopic,

shiny flakes that are optically opaque (> 10 mm) (Figure 1 A and B). It is not clear whether the partial pressure of reactive intermediates in the gas phase of the reactor plays a role in the formation of TGCN, because the overall condensation mechanism is accompanied by a release of ammonia (Figure S1). After cooling, TGCN films can be separated easily from the solidified PTI/Br containing salt block through a simple water washing. The microcrystalline, yellow/brown powder of PTI/Br is suspended in the resulting slurry, while the TGCN flakes float on the surface and can be obtained in pure form by sedimentation and filtration (Figure 1 A and B). TGCN grown at the solid–liquid interface also adheres to the quartz glass support in the reactor and can be peeled, or scratched, away from the surface with relative ease (Figure S2, C).

We used a combination of transmission electron microscopy (TEM) and scanning force microscopy (SFM) to image the materials and to probe the lateral order of TGCN, and to corroborate historical structural predictions.^[7b] Thin sheets of TGCN down to approximately three atomic layers were obtained by mechanical cleavage. TEM images show a hexagonal 2D honeycomb arrangement with a unit-cell of 2.6 Å (Figure 1 E, and Figure S3 D). Under our imaging

conditions, the positions of the three coordinated nitrogen atoms of a triazine-based lattice show up as bright areas (Figure 1 D and E and Figure S3). In the stacking model that best reproduces our TEM data (Figure 1 C), the trigonal voids opened up by the three interlinked triazine units are covered by a staggered, graphitic arrangement of subsequent TGCN layers. Unfortunately, no monolayers of TGCN could be obtained by mechanical cleaving. The hexagonal in-plane pattern seen by SFM ($a = b = 2.78 \pm 0.14$ Å and $\alpha = 59.2 \pm 2.4^\circ$) confirms this repeat of localized electron density (Figure 1 C, and Figure S4). We suggest that this lateral repeat corresponds to a hexagonal grid with electronegative nitrogen atoms at its nodes, as seen for the lateral unit cell of TGCN (Figure 1 F, and Figure S3). Exhaustive scanning electron microscopy (SEM) imaging and energy-dispersive X-ray (EDX) spectroscopy show a homogenous, lamellar sample morphology and a composition that comprises carbon and nitrogen (Figures S5 and S6) in a C_3N_4 ratio (Table S1). ^{13}C and ^{15}N solid-state NMR spectra (Figure 1 G and H, and

Figure S7), X-ray photoelectron spectra (XPS) of the C 1s and N 1s regions (Figure S8), and electron energy loss spectroscopy (EELS) (Figure S9) suggest a material comprised from carbon and nitrogen with the correct hybridization states for an aromatic triazine (C_3N_3)-based structure. The low signal-to-noise ratio in the NMR spectra results from a lack of coupling 1H environments—as corroborated by elemental analysis (Table S1), and also from a degree of structural disorder. The quality of the spectra does not allow definitive structural identification, but data suggest one broad ^{13}C resonance and two groups of ^{15}N peaks, both of which are consistent with the structural model of a planar triazine-based material. X-ray diffraction (XRD) analysis confirmed the purity of TGCN, and no diffraction peaks were observed that could be ascribed to the starting material, the salt melt, nor the PTI/Br, which contains heavy halide scatterers (Figure 1 I, and Figure S10). Following the structural leads from TEM and SFM, we assumed the historical model of “g- C_3N_4 ”^[7b] as an initial guess for structural refinement. This structure is based on a staggered AB arrangement of sheets of nitrogen-bridged triazines (C_3N_3), analogous to graphite (Figure 1 C), and gave reasonable experimental values from Le Bail fitting and constrained structural refinement ($a = 5.0415(10)$ Å, $c = 6.57643(31)$ Å, space group $P\bar{6}m2$, no. 187). Looking at the ab -plane of the refined unit cell, we see a regular grid corresponding to a quarter unit cell giving distances between individual nitrogen atoms of 2.52 Å. The apparent discrepancies in nitrogen–nitrogen distances from TEM (2.60 ± 0.05 Å), SFM (2.78 ± 0.14 Å), XRD (2.52 Å) and DFT (2.39 ± 0.9 Å; min. 2.31 Å, max. 2.66 Å; Figure S13B) are intrinsic to these methods, but they give a good overall agreement of 2.57 ± 0.25 Å. The interlayer spacing of 3.28(8) Å (d_{002}) is slightly shorter than the gallery height of graphite (3.35 Å) (Figure 1 I) and in good agreement with other aromatic, discotic systems. The lack of observable peaks for bulk TGCN did not allow a reliable Rietveld refinement of atom positions, or a confident determination of the possible layer stacking arrangements. However, the initial structural model was used to construct three conceivable stacking possibilities: 1) an eclipsed, AA arrangement, in which consecutive sheets are superimposed over each

other (Figure 2 A); 2) a staggered, graphite-like AB arrangement with one set of triazine (C_3N_3) units from the first layer always superimposed on top of the voids of the second layer (and their neighbors from the first layer always superimposed on the bridging nitrogens from the second layer) (Figure 2 B); and 3) an ABC stacking, where each triazine (C_3N_3) ring is superimposed on a bridging nitrogen followed by a void (Figure 2 C). Simulated TEM images based on these three models were then compared with the experimental TEM data. An ABC arrangement gave the best fit for the thinnest observed sections of TGCN (Figure 2, and Figure S3). However, stacking disorder in thicker parts of the sample is a possibility, as apparent from the broad (002) peak in the XRD pattern (Figure 1 I). This type of disorder between TGCN layers is known for other discotic systems for which stacking is dominated by non-directional π – π interactions.^[17]

The co-planar arrangement of nitrogen-bridged, aromatic triazine (C_3N_3) units enables extended in-plane delocalization of π -electrons along individual sheets of TGCN, and hence

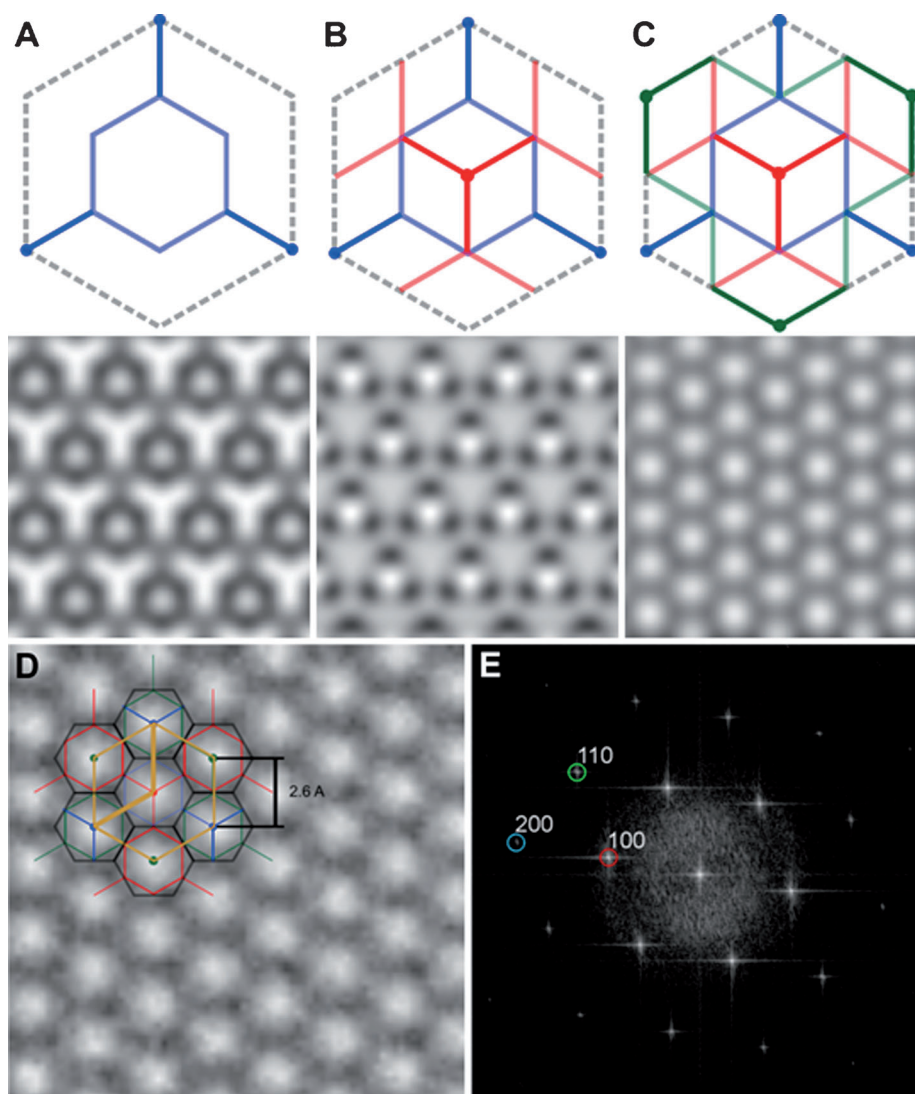


Figure 2. Three possible stacking arrangements of TGCN: A) eclipsed AA, B) staggered AB, C) and ABC, with their respective calculated images below. D) TEM image of TGCN, and E) corresponding Fourier transform image.

opens up interesting perspectives for electronic applications. The opaque, shiny appearance of bulk TGCN makes optical spectroscopy challenging (Figures S11 and S12). However, the onset of an adsorption edge in the red region of the UV/Vis spectrum is discernible (Figure 3A). Hence, the optical bandgap of TGCN is estimated to be less than 1.6 eV. To corroborate the bandgap properties of TGCN, density functional theory (DFT) calculations were performed using a fully non-local functional that includes van der Waals interaction and specifically targets weakly bonded layered systems, (Figure 3B and C and Figure S13, A)^[18] starting with the original model for “g-C₃N₄”.^[7b] The resulting equilibrium structure shows a corrugation of triazine (C₃N₃)-based sheets as observed in previous findings (Figure 3C, and Figure S13A).^[19] While there is evidence in the literature and in the present calculations that the actual g-C₃N₄ structure should be non-planar, the actual extent of corrugation/buckling is difficult to access, and is discussed in-depth in the Supporting Information. The lowest energy is found for an AB stacking arrangement, and an interlayer binding energy of 17.6 meV Å⁻² with a minimum interlayer separation of 3.22 Å. The energy differences between AA, AB and ABC stacking configurations are small (max. 14 meV/atom), which indicates that different stacking configurations should be possible, as indicated by XRD and TEM. The band structure for a single layer of the equilibrium structure is shown in Figure 3C. The single layer bandgap for a free-standing sheet is about 2.4 eV, and it shrinks to 2.0 eV for an AB-stacking arrangement. Since the lowest-energy transition occurs at the Γ point, TGCN is assumed to be a direct bandgap semiconductor, like polymeric carbon nitride analogues.^[16] A comparison of the calculated electronic band structure with the experimental XPS valence band spectrum shows an excellent agreement up to a binding energy of 20 eV, except for the presence of a feature around 1.0 eV in the theoretical spectrum (Figure 3D). This feature corresponds to 2p orbitals nearly orthogonal to the aromatic plane (Figure S14). Due to very low overlap between the initial p π state and free photoelectron wavefunctions, such orbitals are known to have anomalously low photoionization cross sections in *c*-axis-orientated layered materials, such as graphite^[20] and h-BN.^[21] Thus the absence of this peak in layered TGCN can be rationalized. The calculated valence band spectrum for the unrelaxed, planar structure is significantly different to that observed (Figure S15). Hence, the excellent match between our experimental valence band spectrum and the theoretical spectrum for the relaxed model is more supportive of a corrugated structure. On the whole, combined experimental and computational data, and in particular DFT calculations and XPS measurements, support a corrugated layer structure, although limitations in the various measurement techniques and structural disorder in the TGCN material do not allow us to completely rule out a more planar structure, as found

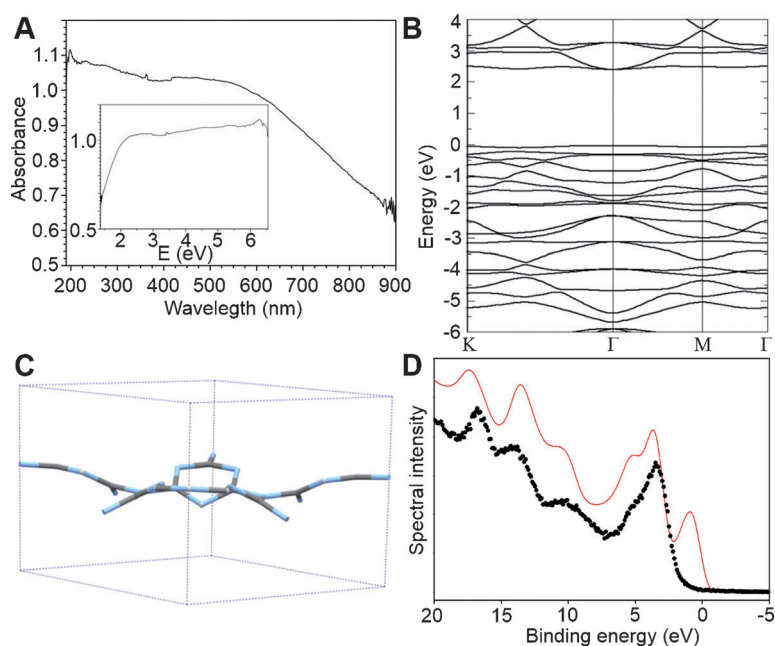


Figure 3. A) UV/Vis diffuse-reflectance spectrum with Kubelka–Munk plot (inset) of TGCN. B) DFT calculated band structure for a single sheet of TGCN. C) Corrugated structure of one layer of TGCN found from DFT calculations. D) XPS spectrum of the valence band region of TGCN (black circles) and calculated XPS plot for the theoretically determined equilibrium structure (red line) (Figure S13).

typically in molecular nitrogen-substituted triazines (Figure S18).

From UV/Vis measurements and the correlation of DFT and XPS results, we deduce that TGCN has a bandgap of between 1.6 and 2.0 eV, which places it in the range of small bandgap semiconductors such as Si (1.11 eV), GaAs (1.43 eV), and GaP (2.26 eV).^[22]

In summary, a triazine-based, graphitic carbon nitride that was predicted in 1996 has now been successfully synthesized. Because of its direct, narrow bandgap, TGCN provides new possibilities for post-silicon electronic devices. In particular, the crystallization of semiconducting TGCN at the solid–liquid interface on insulating quartz offers potential for a practically relevant device-like adaptation.

Received: February 13, 2014

Revised: March 28, 2014

Published online: May 18, 2014

Keywords: carbon nitride · graphene · semiconductor · thin films

- [1] K. S. Novoselov, D. Jiang, F. Schedin, T. J. Booth, V. V. Khotkevich, S. V. Morozov, A. K. Geim, *Proc. Natl. Acad. Sci. USA* **2005**, *102*, 10451–10453.
- [2] a) S. Hertel, D. Waldmann, J. Jobst, A. Albert, M. Albrecht, S. Reshanov, A. Schöner, M. Krieger, H. B. Weber, *Nat. Commun.* **2012**, *3*, 957; b) A. K. Geim, K. S. Novoselov, *Nat. Mater.* **2007**, *6*, 183–191; c) B. Standley, W. Bao, H. Zhang, J. Bruck, C. N. Lau, M. Bockrath, *Nano Lett.* **2008**, *8*, 3345–3349.

- [3] a) A. S. Mayorov, R. V. Gorbachev, S. V. Morozov, L. Britnell, R. Jalil, L. A. Ponomarenko, P. Blake, K. S. Novoselov, K. Watanabe, T. Taniguchi, A. K. Geim, *Nano Lett.* **2011**, *11*, 2396–2399; b) S. Hertel, F. Kisslinger, J. Jobst, D. Waldmann, M. Krieger, H. B. Weber, *Appl. Phys. Lett.* **2011**, *98*, 212109; c) Y. Zhang, Y.-W. Tan, H. L. Stormer, P. Kim, *Nature* **2005**, *438*, 201–204.
- [4] F. Schwierz, *Nat. Nanotechnol.* **2010**, *5*, 487–496.
- [5] a) T. Ohta, A. Bostwick, T. Seyller, K. Horn, E. Rotenberg, Science **2006**, *313*, 951–954; b) J. B. Oostinga, H. B. Heersche, X. L. Liu, A. F. Morpurgo, L. M. K. Vandersypen, *Nat. Mater.* **2008**, *7*, 151–157; c) C. Berger, Z. Song, X. Li, X. Wu, N. Brown, C. Naud, D. Mayou, T. Li, J. Hass, A. N. Marchenkov, E. H. Conrad, P. N. First, W. A. de Heer, *Science* **2006**, *312*, 1191–1196; d) F. Withers, M. Dubois, A. K. Savchenko, *Phys. Rev. B* **2010**, *82*, 073403.
- [6] a) K. F. Mak, C. Lee, J. Hone, J. Shan, T. F. Heinz, *Phys. Rev. Lett.* **2010**, *105*, 136805; b) B. Radisavljevic, A. Radenovic, J. Brivio, V. Giacometti, A. Kis, *Nat. Nanotechnol.* **2011**, *6*, 147–150.
- [7] a) A. Y. Liu, R. M. Wentzcovitch, *Phys. Rev. B* **1994**, *50*, 10362–10365; b) D. M. Teter, R. J. Hemley, *Science* **1996**, *271*, 53–55.
- [8] E. Kroke, M. Schwarz, *Coord. Chem. Rev.* **2004**, *248*, 493–532.
- [9] J. Kouvetakis, A. Bandari, M. Todd, B. Wilkens, N. Cave, *Chem. Mater.* **1994**, *6*, 811–814.
- [10] a) T. Sekine, H. Kanda, Y. Bando, M. Yokoyama, K. Hojou, *J. Mater. Sci. Lett.* **1990**, *9*, 1376–1378; b) A. Thomas, A. Fischer, F. Goettmann, M. Antonietti, J. O. Muller, R. Schlogl, J. M. Carlsson, *J. Mater. Chem.* **2008**, *18*, 4893–4908.
- [11] M. R. Wixom, *J. Am. Ceram. Soc.* **1990**, *73*, 1973–1978.
- [12] M. J. Bojdys, J.-O. Mueller, M. Antonietti, A. Thomas, *Chem. Eur. J.* **2008**, *14*, 8177–8182.
- [13] a) B. V. Lotsch, W. Schnick, *Chem. Mater.* **2005**, *17*, 3976–3982; b) X. Li, J. Zhang, L. Shen, Y. Ma, W. Lei, Q. Cui, G. Zou, *Appl. Phys. A* **2009**, *94*, 387–392.
- [14] B. V. Lotsch, W. Schnick, *Chem. Eur. J.* **2007**, *13*, 4956–4968.
- [15] a) S. Y. Chong, J. T. A. Jones, Y. Z. Khimyak, A. I. Cooper, A. Thomas, M. Antonietti, M. J. Bojdys, *J. Mater. Chem. A* **2013**, *1*, 1102–1107; b) E. Wirnhier, M. Döblinger, D. Gunzelmann, J. Senker, B. V. Lotsch, W. Schnick, *Chem. Eur. J.* **2011**, *17*, 3213–3221.
- [16] X. C. Wang, K. Maeda, A. Thomas, K. Takanabe, G. Xin, J. M. Carlsson, K. Domen, M. Antonietti, *Nat. Mater.* **2009**, *8*, 76–80.
- [17] A. P. Cote, A. I. Benin, N. W. Ockwig, M. O’Keeffe, A. J. Matzger, O. M. Yaghi, *Science* **2005**, *310*, 1166–1170.
- [18] T. Bjorkman, *Phys. Rev. B* **2012**, *86*, 165109.
- [19] a) Y. Miyamoto, M. L. Cohen, S. G. Louie, *Solid State Commun.* **1997**, *102*, 605–608; b) D. T. Vodak, K. Kim, L. Iordanidis, P. G. Rasmussen, A. J. Matzger, O. M. Yaghi, *Chem. Eur. J.* **2003**, *9*, 4197–4201.
- [20] U. Berg, G. Drager, O. Brummer, *Phys. Status Solidi B* **1976**, *74*, 341–348.
- [21] E. Tegeler, N. Kosuch, G. Wiech, A. Faessler, *Phys. Status Solidi B* **1979**, *91*, 223–231.
- [22] B. G. Streetman, B.S., *Solid State Electronic Devices*, 6 ed., Pearson, **1999**.